18

Molecular Dynamics Simulation and Conductivity Mechanism in Fast Ionic Crystals Based on Hollandite $Na_xCr_xTi_{8-x}O_{16}$

Kien Ling Khoo[1,2] and Leonard A. Dissado[2]
[1]*Invion Technologies Sdn Bhd*
[2]*Engineering Department, University of Leicester, Leicester*
[1]*Malaysia*
[2]*UK*

1. Introduction

Fast ion conductors are keystone materials in the development of high performance solid oxide fuel cells and solid electrolytes. In spite the significant contributions in this area a fundamental understanding of the correlation between crystal structure and ionic conductivity is still lacking. In this chapter we report our recent computer simulation results on Hollandite ionic crystals. The objective of this work is to provide the structural parameters which will lead to the design and synthesis of high performance ionic conductors.

Hollandites are ionic crystals of a rather unusual kind, in which the ions of one type are in a disordered and highly mobile state (Dixon & Gillan, 1982). Such materials often have rather special crystal structures in that there are open tunnels or layers through which the mobile ions may move (West, 1988). Their crystal structure corresponds to a family of compounds of general formula $A_xM_{4-x}N_yO_8$. The basic formula of the Hollandite structure used in the research is $Na_x(Ti_{8-x}Cr_x)O_{16}$, (Michiue & Watanabe, 1995a, 1996). The chromium and titanium ions are randomly placed in unit cells according to the relative proportions of titanium and chromium ions with a corresponding amount of sodium ions to compensate for the smaller charge on the chromium ions (+3) compared to the titanium ions (+4).

The main interest of this Na-priderite is its structure as a promising (1-D) Na ion conductor (Michiue & Watanabe, 1995b). Priderites, titania-based hollandites, are typical one-dimensional ion conductors in which the 1-D tunnels are available for transport of cations in the tunnel (hereafter the "tunnel ion") (Michiue & Watanabe, 1995a). Priderites are generally represented by $A_xM_yTi_{8-y}O_{16}$, where A is the alkali or alkaline earth ions and M, di- or trivalent cations (Michiue & Watanabe, 1995a; A. Byström & A.M. Byström, 1950). The host structure for the hollandite being used mainly consists of titanium ions and oxygen ions. These titanium ions are each octahedrally bonded to six oxygen ions. Two such octahedra are joined by sharing an edge, and these doubled groups share further edges above and below to form extended double strings parallel to the growth axis. Four such double strings are joined by corner sharing to form a unit tunnel. The sodium ions are situated in the

tunnels, and each is ionically bonded to eight oxygen ions of the host structure at the corners of a slightly distorted cube. These cubes form a string of ion cages along the axis of a tunnel, and since not all cages have a chromium ion in the place of a titanium ion not all cages contain a sodium ion. The availability of vacant sites into which the sodium ion can move is what allows ion transport to be possible. A typical hollandite structure is shown in figure 1.

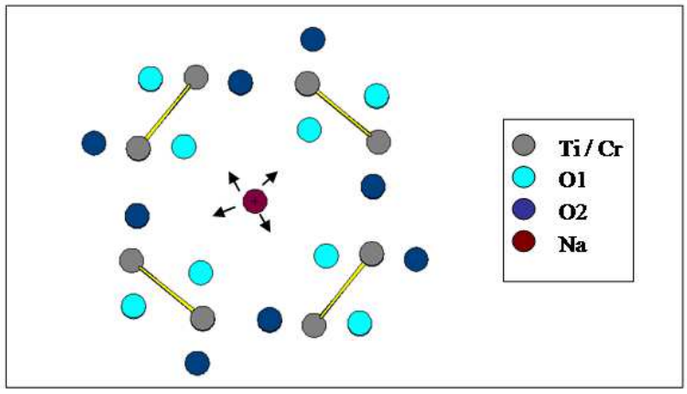

Fig. 1. A typical hollandite structure projected along the c-axis.

The behaviour of the tunnel ion is usually complicated because it interacts not only with the ions in the lattice sites but also with the other tunnel ions. The main two interactions are Lennard-Jones potential for the short range and Coulomb potential for the long range. Although the ions at the lattice sites give a potential surface for the tunnel ions, which the sodium ions move on, the interactions with other sodium ions in the tunnel is a many body problem like a liquid.

Herein, we investigate the response of the sodium ions under the effect of electric field. The dielectric behaviour of the hollandites is typically studied in the low frequency region [10^2-10^9 Hz]. Dryden and Wadsley (Dryden & Wadsley, 1958), in the first publication on the structure and electrical properties of a hollandite, reported the existence of a dielectric relaxation in several BaMg hollandites, which had a maximum absorption at room temperature in the radio frequency region of the spectrum (10^5-10^8 Hz). They reported that the dielectric absorption was only detected when the electric field was in the direction of the tunnel. The activation energy for the peak frequency representing the energy barrier to be overcome for ion displacement was found to be 0.17eV. Cheary and Dryden (Cheary & Dryden, 1991) reported that the mobility of the tunnel ion in Ba hollandite is very low except in limited regions and the activation energy that they obtained is 0.24eV. Activation energies of the order 0.05eV claimed by others was only detected in some samples with the presence of impurity TiO_2 as a second phase. Since then there have been further experimental work on the dielectric properties of hollandites published by Singer et al (Singer et al., 1973). Yoshikado et al (Yoshikado et al., 1982) emphasize the loss factor (ε") at low frequencies which increases with decreasing frequency and usually depends on frequency as f^{-n} where $n<1$. Jonscher (Jonscher, 1983) concluded that the response of fast ion conductors follows the "universal law" for the charge carriers. He showed that strong low-frequency dispersion occurs at high temperature, 373K, in the hollandite ($K_{1.8}Mg_{0.9}Ti_{7.1}O_{16}$). The behaviour in the high frequency region is not well understood. Michiue and Watanabe (Michiue & Watanabe, 1999) reported that the strong response observed for the imaginary part of the dielectric

permittivity for K-hollandites around 100-300 cm^{-1} ($3x10^{12}$ – $9x10^{12}$ Hz) is due to the vibration of the framework structure. Not much work has been done in investigation for the frequency range around 1.2-70 cm^{-1} ($3.6x10^{10}$ – $2.1x10^{12}$ Hz).

Dissado and Hill (Dissado & Hill, 1983) predicted that particles moving in a flexible local environment experienced a cooperative interaction between the particle and their environment leading to a specific form of dielectric response, the constant phase angle response, $C'(f) \propto C''(f) \propto f^{-p}$. Dissado and Alison (Dissado & Alison, 1993) showed that this form of response included a Poley absorption peak in the far infra-red region of the spectrum. This form of absorption peak was observed by Poley (Poley, 1955), Davies (Davies et al, 1969) and some others (Johari, 2002; Chantry, 1977) in both liquids and solids and was named after Poley. The "liquid-like" hollandite structure is similar in form to the materials in which the Poley peak is observed, and hence such a peak can be expected. The theories (Dissado & Alison, 1993; Poley, 1955) suggest that this peak will be caused by the cooperative librations of the dipole produced by the sodium ions and their environmental counter-charges as the sodium ions displace under the many-body interactions of one another. It is the intention here to use molecular dynamics simulations to see if the predicted Poley absorption will be produced by such motions even in the absence of vibrations and flexible displacement in the surrounding crystal.

2. Molecular dynamics (MD) simulation

Molecular dynamics (MD) simulations technique has been used in this research to perform the atomistic calculations, of frequency dependent electrical conductivity in $Na_x(Ti_{8-x}Cr_x)O_{16}$, (x = 1.7). MD simulation is generally carried out to compute the motions of individual molecules in models of solids, liquids and gases. The key idea is motion, which describes how positions, velocities, and orientation change with time (Haile, 1992). The MD simulation method is carried out in such a way that atoms are represented by point particles and the classical (Newton) equations of motion, "force equals mass times acceleration or F = ma" are integrated numerically. The motions of these large numbers of atoms are governed by their mutual interatomic interaction. MD simulations are limited largely by the speed and storage constraints of available computers. Hence, simulations are usually done on system containing 100-1000 particles, with a time step of $1x10^{-15}$ s. This technique for simulating the motions of a system of particles when applied to biological macromolecules gives the fluctuations in the relative positions of the atoms in a protein or in DNA as a function of time. Knowledge of these motions provides insights into biological phenomena. MD is also being used to determine protein structure from NMR, to refine protein X-ray crystal structures faster from poorer starting models, and to calculate the free energy changes resulting from mutation in proteins (Karpus & Petsko, 1990).

The construction of the molecular dynamics model involved mainly model development and the use of the Molecular Dynamics simulation technique to solve the equation of motion iteratively. In model development, firstly the interaction between ions and the interaction between ion and environment have to be defined. The interaction between ions comprises three components: Lennard-Jones potential, Coulomb potential and Van der Waals' attraction. The rigid lattice approximation is being used in the simulation. This describes the interaction between the ions and the environment. In the rigid lattice approximation only the tunnel ions are allowed to displace from their equilibrium position. The environment

ions still give an interaction with the tunnel ions, i.e. they produce a constant potential surface for the tunnel ions. The tunnel ions interact with one another and are allowed to displace. After this has been done, the equations of motion are developed. A program, Gretep (LMGP-Suite Suite of Programs for the interpretation of X-ray Experiments) is used to generate the positions of all the ions by keying in parameters such as space group, unit cell dimensions, atomic parameters and etc. Then titanium ions are replaced by chromium ions randomly placed in unit cells along the tunnel according to the relative proportions of titanium and chromium. A tunnel ion, which is the sodium ion, is added to the model structure for every chromium ion, in order to preserve charge neutrality.

2.1 Modeling of ion-ion interactions

The molecular interactions are based on the intermolecular potential energy function. The total potential energy between two ions is the sum of the Lennard-Jones potential and Coulomb potential (West, 1988),

$$V(r) = \frac{\lambda}{r^p} \pm \frac{e^2}{4\pi\varepsilon_0 r} \tag{1}$$

where p is about 10 and the values for λ are different for different ion-pairs, e is the electron charge and r is the distance between two ions. The values for lambda for each ion-pair have to be found for the calculations of the equations of force. The method used is presented elsewhere (Khoo, 2003; Dissado and Khoo, 2006; Khoo et al., 2004, 2007). The relationship between the tunnel system and its surroundings is defined by using boundary conditions. These describe the interactions between the molecules with their surroundings. Rigid lattice approximation has been used in the simulation to simplify the simulation process and to reduce the simulation executable time. Rigid lattice approximation is done in such a way that only the tunnel ions, which are the sodium ions, are free to displace. All other ions in the lattice sites would remain static. However, there will still be interaction between sodium ions and the ions in the lattice sites.

Reflective boundary conditions are used at the two ends of the tunnel. Rebound is a special type of collision involving a direction change; the result of the direction change is a large velocity change. Collisions in which particles rebound with the same speed are known as elastic collisions. Thus, the velocity of the ion that bounds back from the boundary should have the opposite sign and equal in magnitude with that velocity of ion which hits the boundary. The angle of the velocity hitting the boundary is the same as the angle leaving the boundary. Force is the derivative of potential energy. Therefore, the component of the force along the a-axis is given by equation 2.

$$F_a = -\frac{dV(r)}{da} = \frac{dr}{da}\frac{\lambda p}{r^{p+1}} \mp \frac{dr}{da}\frac{e^2}{4\pi\varepsilon_0 r^2} \tag{2}$$

$$r = \sqrt{(Aion1 - Aion2)^2 + (Bion1 - Bion2)^2 + (Cion1 - Cion2)^2} \tag{3}$$

$$\frac{dr}{da} = \frac{|\, Aion1 - Aion2\,|}{r} \tag{4}$$

where |Aion1 – Aion2| is the absolute value of the displacement in a-axis for ion1 and ion2 and r is the distance between ion1 and ion2. The expressions for the component of forces in the b and c-axes are equivalent in form. The tunnel wall is made up by alternate stacking of two different oxygen-square layers which consist of four oxygen atoms denoted O1 at z = 0 (square-plane) and four oxygen atoms denoted O2 at z = 0.5 (cavity). The number and the positions of the basic tunnel ions are obtained from the x-ray analysis (Michiue & Watanabe, 1995a). There will be six sodium ions in the seven cavities, in other words in the 14 oxygen-square layers. This is shown in figure 2. The position of the sodium ion will depend on the position of the chromium ion.

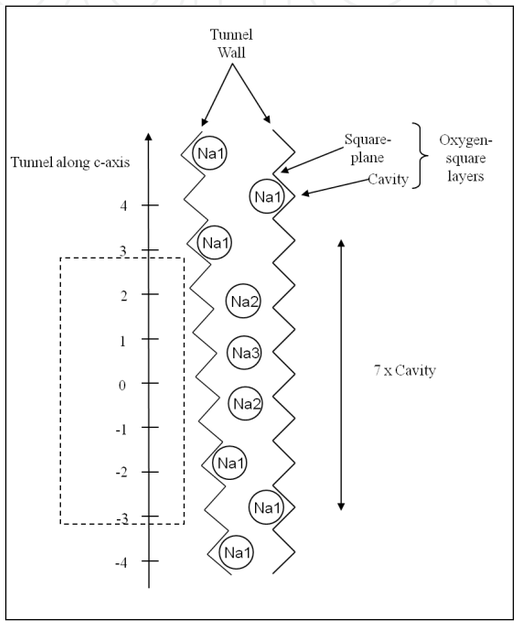

Fig. 2. Schematic representation of a probable local arrangement for sodium ions in the tunnel of $Na_xCr_xTi_{8-x}O_{16}$. In the 7 x Cavity (indicated by the rectangular box), there are six sodium ions.

From figure 2, it is clearly shown that there are three possible equilibrium positions for the sodium ions, Na1 (0.72,0.14,0.5), Na2 (0,0,0.2) and Na3 (0,0,0) (Michiue & Watanabe, 1995a). The three positions are very close to each other and therefore it is impossible for Na ions to occupy these positions simultaneously. The positions for the sodium ion are dependent on the position of the chromium ion. When a titanium ion in the square-plane is substituted by a chromium ion, a sodium ion (either Na2 or Na3) will be placed in the hollandite model as shown in the figure 3. The site of the chromium ion is chosen randomly from the titanium ions in the four corners, A, B, C or D. The Na2 and Na3 differ slightly in their position along the c-axis. The atomic parameters for Na2 and Na3 in c-axis or z-axis shown in figure 3 are 0.2 and 0 respectively. When a titanium ion in the cavity is substituted by a chromium ion, there will be four possible positions for the sodium ion (Na1). The chromium ion is chosen randomly from the titanium ions in the four corners, A, B, C or D. The sodium ion preferentially resides at an interstitial site within the same unit cell that contains a chromium ion (Michiue & Watanabe, 1996) shown by the arrow in figure 3. In this work, 24 sodium ions have been considered. Therefore, four sets of the six sodium ions shown in figure 2 are stacked up together to form a

longer tunnel. C++ is used as a tool to carry out the molecular dynamics simulation, to perform the complicated calculations and to store the required results in the specified text files. A total of five C++ programs have been written and the flow chart is shown in figure 4. Details of the calculations can be found in reference (Khoo, 2003).

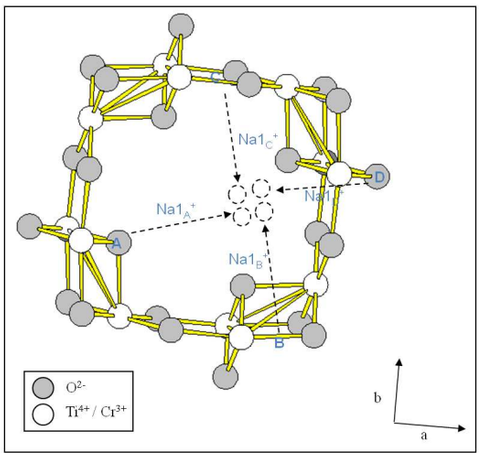

Fig. 3. Hollandite model projected slightly off the c-axis to give a clearer view of the 3-dimensional structure. When Ti_A^{4+} is replaced by Cr^{3+}, the preferable location for the $Na1_A^+$ ions is shown by the arrow, a similar situation is found for Ti_B^{4+}, Ti_A^{4+} & Ti_D^{4+} as shown by $Na1_B^+$, $Na1_C^+$ and $Na1_D^+$.

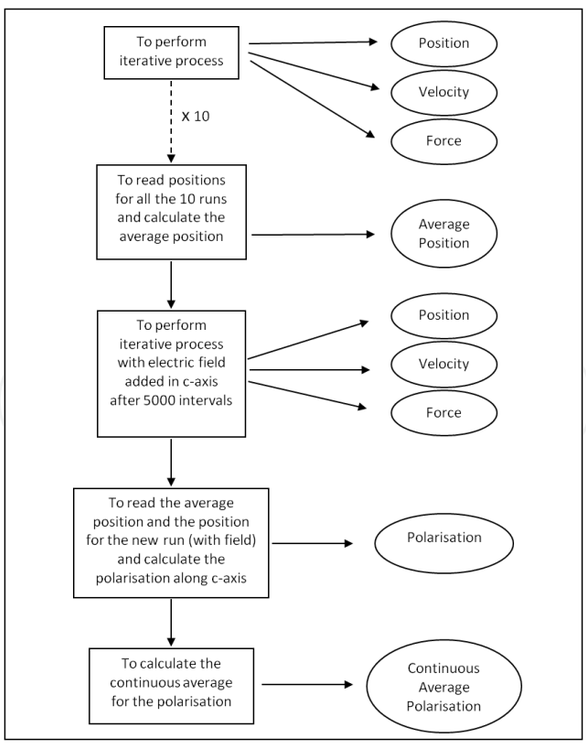

Fig. 4. Flow chart showing the five program codes written to perform the MD simulation, to carry out the complicated calculations and to generate the data required in text files.

3. Results

3.1 Position of sodium ions in c-axis without applied field

After ten runs have been carried out with different initial velocities for the individual sodium ions with their average value being set by the defined temperature, the average positions for each of the sodium ions in the c-axis are then calculated. Figure 5a shows the average position for the first six sodium ions along the c-axis with the initial conditions of 273K, 100000 intervals and time step=10^{-15}s. This gives a good comparison of the positions of the sodium ions throughout the 100000 intervals. The sodium ions only vibrate in their equilibrium positions depending upon where their equilibrium positions were. For example, the sixth sodium ion (pink) only vibrates around the cavity it belongs to.

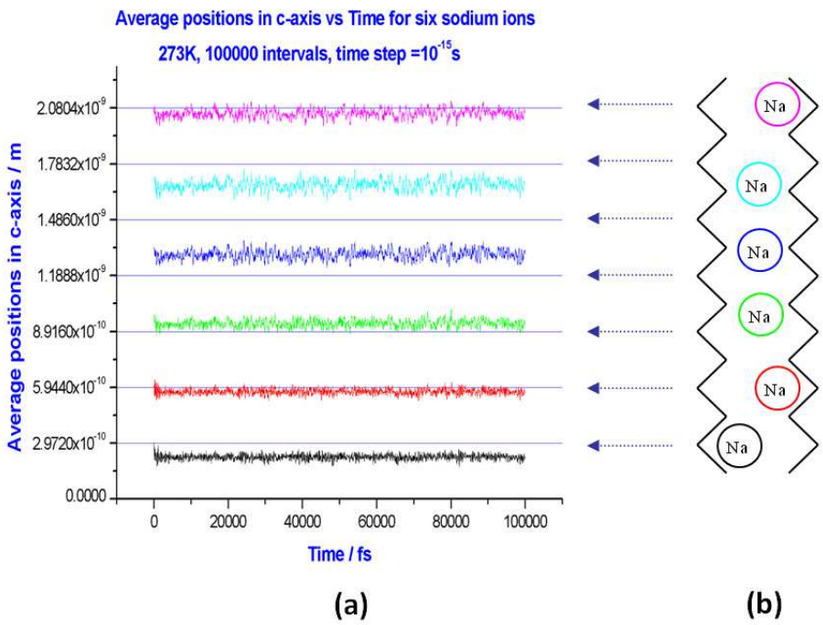

Fig. 5. (a) The average position along the c-axis for the first six sodium ions (b) The arrangement for the first six sodium ions in the tunnel. The arrows show the alignment of the cavities in the tunnel and the graphs.

3.2 Position of sodium ions in c-axis with applied field

An electric field in the range of 7.43MV/m to 74.3GV/m was applied along the c-axis to the hollandite model at the 5001th time interval. The initial conditions for the results shown below were temperature=273K, time step=10^{-15}s, 100,000 intervals and electric field=743MV/m. Figure 6 shows the positions of the first six sodium ions as a function of time. Over the initial 5000 intervals, which was in the absence of the electric field, the sodium ions just vibrate around their equilibrium positions. Starting from 5001th intervals, the positions of the sodium ions change dramatically. For example, the sixth sodium ion (pink) moved to the next cavity at some points and then back to the original cavity and then to the next cavity again.

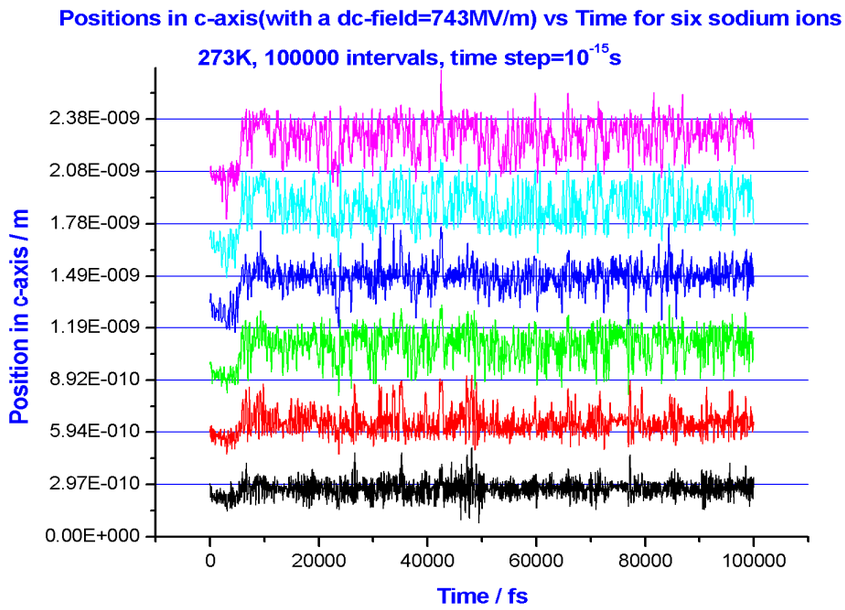

Fig. 6. Position of the first six sodium ions in c-axis when electric field of 743MV/m was applied along the c-axis to the hollandite model at 5001th time interval.

3.3 The polarisation

The polarisation along the c-axis was calculated for a range of electric fields and temperatures. Figure 7 shows the polarisation as a function of time. Over the initial 5000

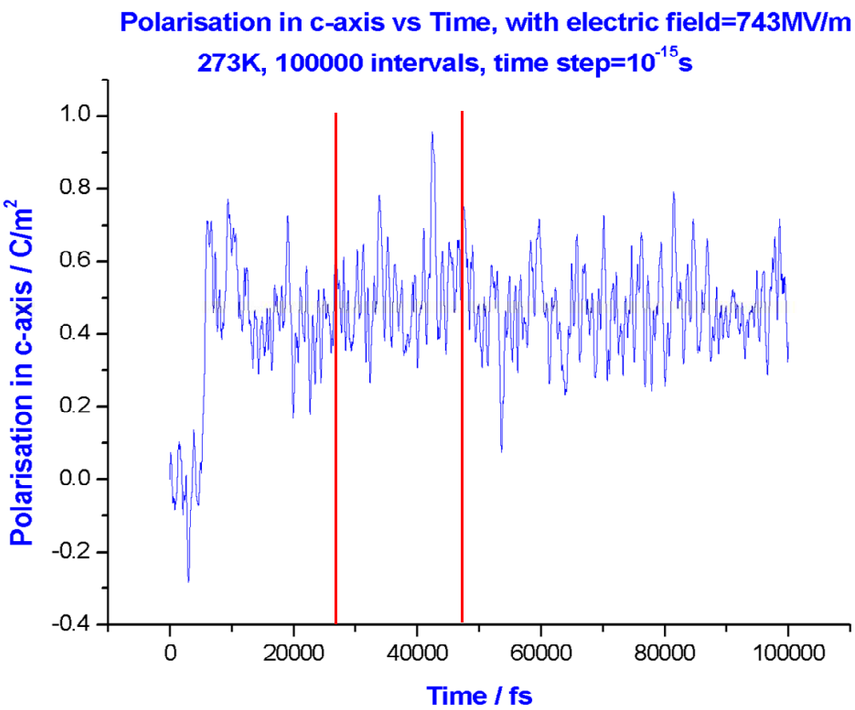

Fig. 7. The polarisation in c-axis with an applied field of 743MV/m as a function of time.

intervals, the polarisation tends to fluctuate around zero. Once the electric field is applied at 5001th interval, the polarisation increases rapidly to around 0.7 C/m² and after that sudden increase, the polarisation remains at an average of that value for the rest of the time intervals. The results under different electric field are similar, but a smaller field gives a smaller polarisation. A running average of the polarisation was taken over 100 intervals and only the results starting from 5001th intervals are taken into account. This is because the results of interest are those under the effect of electric field.

Figure 8 gives the continuous average for the polarisation as a function of time. The plot obtained was not as noisy as the polarisation plot shown in figure 7, as the running average over 100 intervals eliminates vibration periods at 10^{-13} s and shorter.

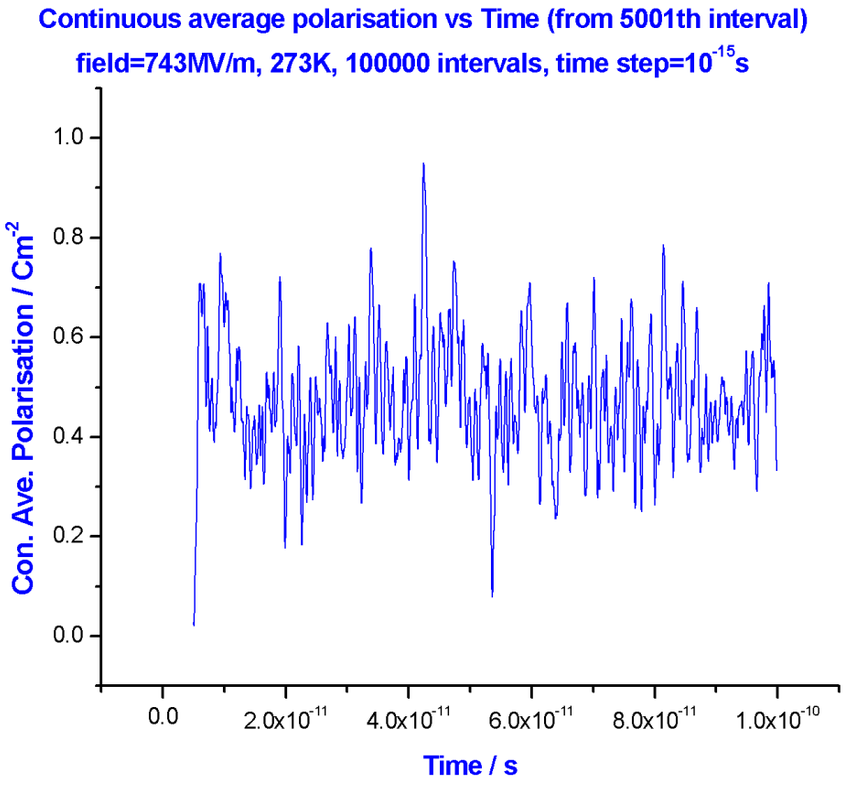

Fig. 8. Continuous average for the polarisation with an applied field of 743MV/m as a function of time.

3.4 Fast Fourier Transform (FFT) – Susceptibility

The Fast Fourier Transform (FFT) is performed in order to calculate the behaviour of the hollandite model in the frequency domain. The continuous average of the polarisation is imported to "Origin" program. A graph of polarisation versus time is plotted. Only the data between the 5001th and 100000th gives the polarisation since the electric field is switched on at the 5000th interval. The time derivative of the polarisation is then obtained via the program, and is plotted. The one-sided Fourier Transform of $(dP/dt)/Ee_0$ gives the frequency dependent dielectric susceptibility for comparison with experiment. The easier way to carry out the FFT in "Origin" software is by performing FFT on the dP/dt, the

results obtained are then divided by electric field, E and permittivity of free space, ε_0 to give the real and imaginary parts of the susceptibility. The FFT mathematical description is shown as follows:

$$X[k] = \sum_{n=0}^{N-1} x[n] \exp(-i2\pi F_k n) \tag{5}$$

with $F_k = k / N$, where FFT transforms x[n] into X[k]. The input data set is x[n] with index n in the range $0 \le n \le N-1$. It is easy to convert the index into "time" $t = n\tau$, where τ is the (time) interval, and $F_k = k / N$ into "frequency" $f_k = k / N\tau$.

Curve fitting is important, as it will give the best curve fit to the graph obtained. Firstly, the Real and Imaginary part of the susceptibility (the results generated by the FFT from the previous section) are plotted against frequency in two different graphs. This is to ease the fitting procedure as the two graphs are of different shape hence two different fitting functions are defined. If the results exhibit relaxation behaviour, then we would expect the loss peak to be characterised by power law frequency dependencies above and below the peak frequency.

If the results show a resonance character then we have to fit them to an appropriate expression. Two types of expressions are commonly used.

1. A Gaussian absorption function. This relates to a superposition of oscillator resonances with each oscillator vibrating independently of one another at a specific frequency, with the probability of a given frequency being defined by the Gaussian function. In our case the vibrations are those of the sodium ions, and these are not independent of one another, so the Gaussian form should not apply.
2. A Lorentzian function. This relates to an oscillator whose oscillations are damped by interaction with its surroundings. In our case we can think of a chosen sodium ion oscillator as being damped by its interaction with the other sodium ions. So the function may approximate to our situation. However, the other sodium ions also contribute to the response via group motions, so the Lorentzian is at the best an approximation to our hollandite model. Nonetheless the Lorentzian will be fitted to the data to see how good an approximation it is, and to determine in what respect it fails.

The real part of the susceptibility given in term of x (frequency) and w (damping factor) is shown in equation 6:

$$y = \frac{4A}{\pi} \frac{x_c - x}{4(x_c - x)^2 + w^2} \tag{6}$$

The imaginary part of the susceptibility given in term of x and w is shown in equation 7:

$$y = \frac{2A}{\pi} \frac{w}{4(x_c - x)^2 + w^2} \tag{7}$$

x_c, w and A are the parameters used for the resonant frequency, full width at ½ maximum and amplitude factor respectively.

The real part of the susceptibility, $\chi'(f)$ and the imaginary part of the susceptibility, $\chi''(f)$ were then obtained by dividing the results generated from the FFT by the applied field and

permittivity of free space. The χ' (f) and χ''(f), obtained from the FFT, are plotted as a function of frequency (f) as shown in figure 9.

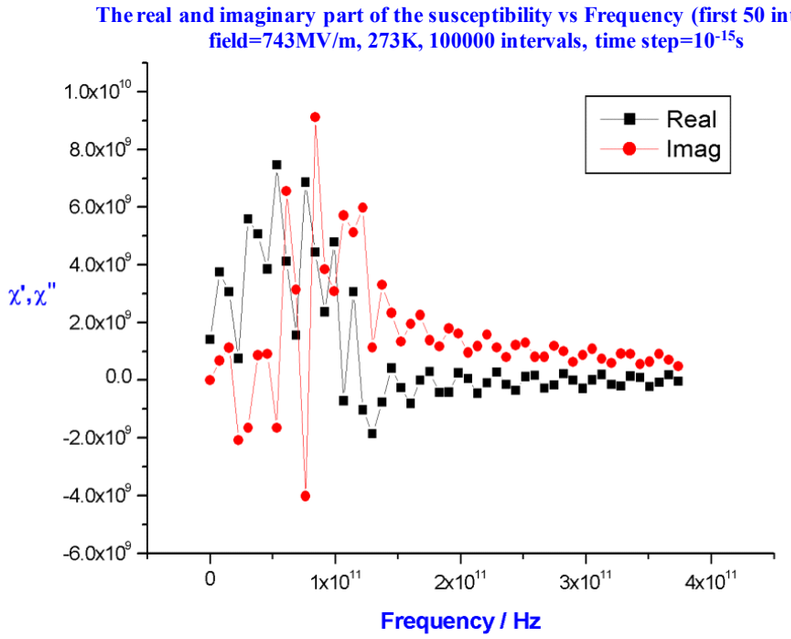

Fig. 9. The real and imaginary parts of the susceptibility as a function of frequency with an electric field of 743MV/m.

The simulation was run for 100ps (100000 x 10^{-15}s), which correspond to 10^{10} Hz. The susceptibility at frequencies below $4x10^{10}$Hz is unreliable as it relates to FFT extrapolations to regions, which are not consistent with the largest time (10^{-10}s) reached by the computation. At the higher frequency range, the smoothing process has removed the frequency higher than $2x10^{11}$ Hz; hence, frequency higher than $2x10^{11}$ Hz is similarly unreliable. Figure 9 shows χ'(f) and χ''(f) as a function of frequency. χ'(f) goes to a positive value, then drops to a negative value and then starts to fluctuate around a smaller negative value. χ''(f) shows a peak at about $1x10^{11}$ Hz and the frequency of the peak lies about half way along the slope of the χ'(f). From the overall non-monotonic behaviour of χ'(f), it is clear that the response is not that of a dielectric relaxation; hence the curve fitting to the Lorenzian function which is the resonance response would have to be carried out.

3.5 Depolarisation

An electric field was applied to the hollandite model at the start of the simulation for 5000 intervals. Then the field was switched off at 5001th interval. The depolarisation, continuous average for the depolarisation, FFT and curve fitting were obtained similarly to the procedures outlined above. Depolarisation was carried out with initial conditions of temperature=297K, time step=10^{-15}s, 100000 intervals and electric field=7.43GV/m. The results of the curve fitting to equations 6 and 7 for χ'(f) and χ''(f) (obtained from the depolarisation) respectively as a function of frequency are shown in the figure 10 and 11 below.

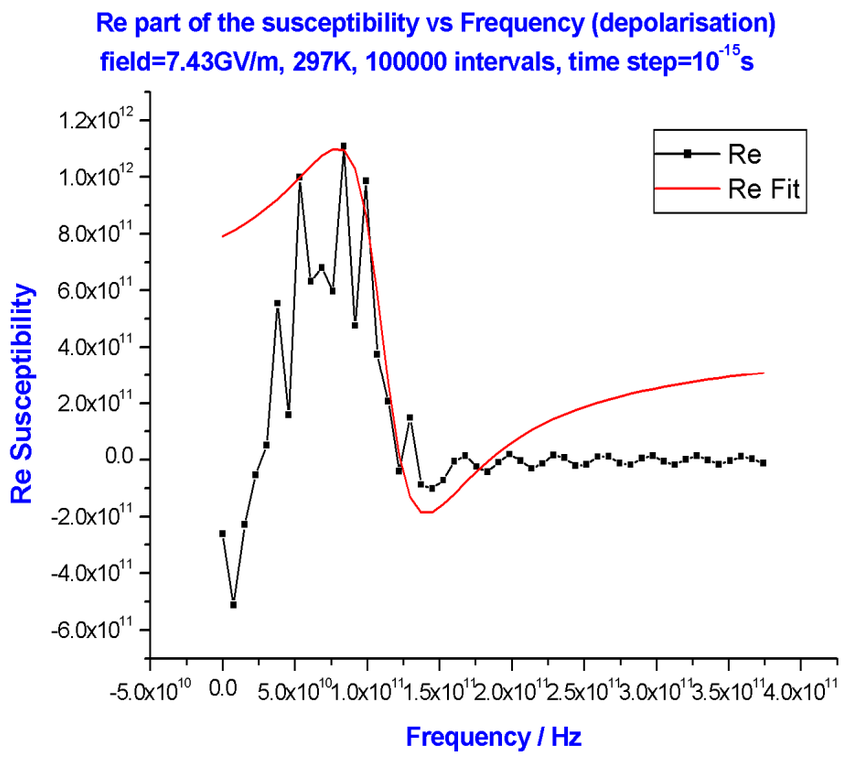

Fig. 10. The $\chi'(f)$ plot with the best fitting curve (red) to equation 6 as a function of frequency.

From figure 10, it is clearly shown that the equation 6 does not fit well to $\chi'(f)$ at all. For a resonance response, the magnitude for the lower frequency range should not be lower than the magnitude in the higher frequency range. Figure 11 shows that the equation 7 does not fit well with the simulation values of $\chi''(f)$ either. The fitted curve fits nicely in the higher frequency range but in the lower frequency range, the gradient of $\chi''(f)$ is much bigger than the fitting curve. It seems that the hollandite model had not reached an equilibrium state when the electric field was taken off. From the figure 12, the $\chi'(f)$ and the $\chi''(f)$ for the polarisation and the depolarisation were different although they should be identical for a linear response. Both the magnitude of the $\chi'(f)$ and $\chi''(f)$ for the depolarisation are bigger than the $\chi'(f)$ and $\chi''(f)$ of the polarisation. The resonance frequency of $\chi''(f)$ for the polarisation is lower compared to the resonance frequency of $\chi''(f)$ for the depolarisation.

3.6 Results obtained at the temperatures of 200K to 373K and with electric fields between 7.43MV/m and 74.3GV/m

The simulation has also been carried out with initial conditions of temperature between 200K and 373K, which were 200K, 250K, 273K, 297K and 373K. At each temperature, six different electric fields were investigated between 7.43MV/m and 74.3GV/m, which were 7.43MV/m, 74.3MV/m, 371.5MV/m, 743MV/m, 7.43GV/m and 74.3GV/m. On each of the results the procedures described in section 3.4 were carried out for the data analysis. The

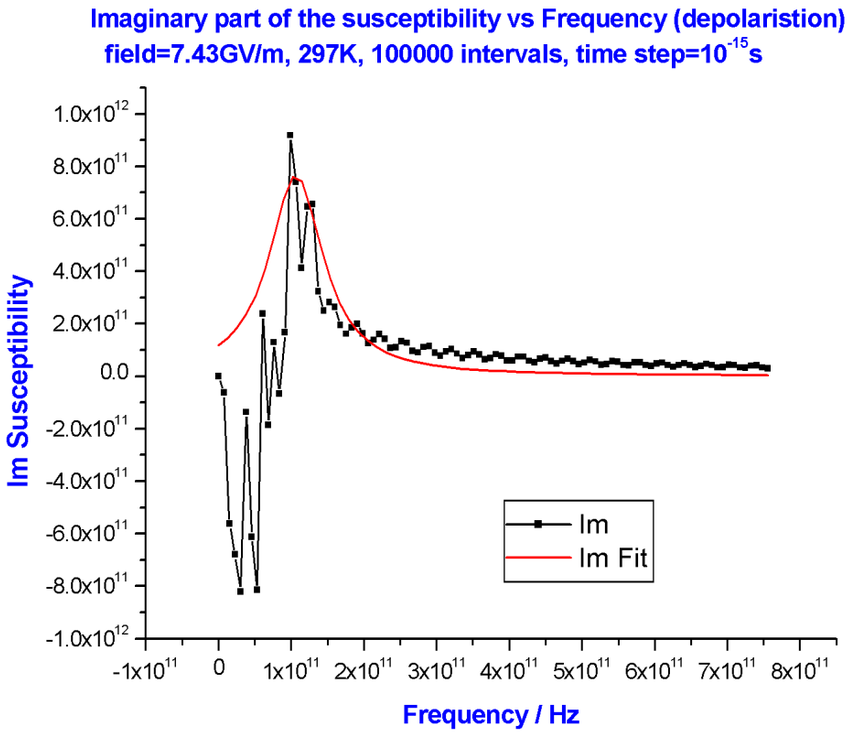

Fig. 11. The $\chi''(f)$ plot with the best curve fitting (red) to equation 7 as a function of frequency.

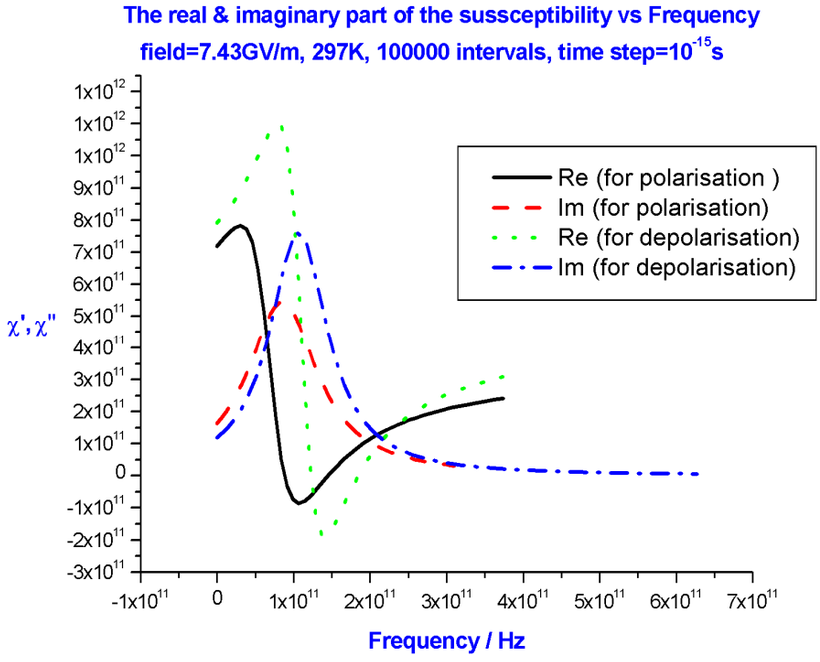

Fig. 12. The results of the curve fitting to equation 6 and 7 for both the $\chi'(f)$ and the $\chi''(f)$ of polarisation and the depolarisation respectively with an electric field of 7.43GV/m.

real part of the susceptibility does not fit well with equation 6. Hence, only the values for the parameters used (x_c, w, A_0) for the imaginary parts of the susceptibility are shown in table 1.

For all five temperatures (200K to 373K), the imaginary parts of the susceptibility (fitted to equation 7) for the electric field in the range of 7.43MV/m to 7.43GV/m show an absorption peak. The magnitude of the absorption peak differs with temperature and electric field. At an electric field of 74.3GV/m the polarisation was found to oscillate between two values. The time period can be determined from the polarisation plot. An example of the polarisation plot at 200 K is given in figure 13 which is just a part of the polarisation plot (5500^{th}-5530^{th} intervals) with initial conditions of 200K, 74.3GV/m and time step=10^{-15}s. The polarisation plot of 100000 intervals is the replication of the plot shown above. There are two and a half oscillations highlighted between the two red lines in the figure and the period of the oscillation is $4x10^{-15}$s. The time step for the simulation is 10^{-15}s, and the period of the oscillation is four times the time step. Therefore, at high electric field, all the sodium ions were driven by this force field to move as a group and they show a single frequency vibration caused by reflections from the tunnel boundaries according to the input boundary conditions.

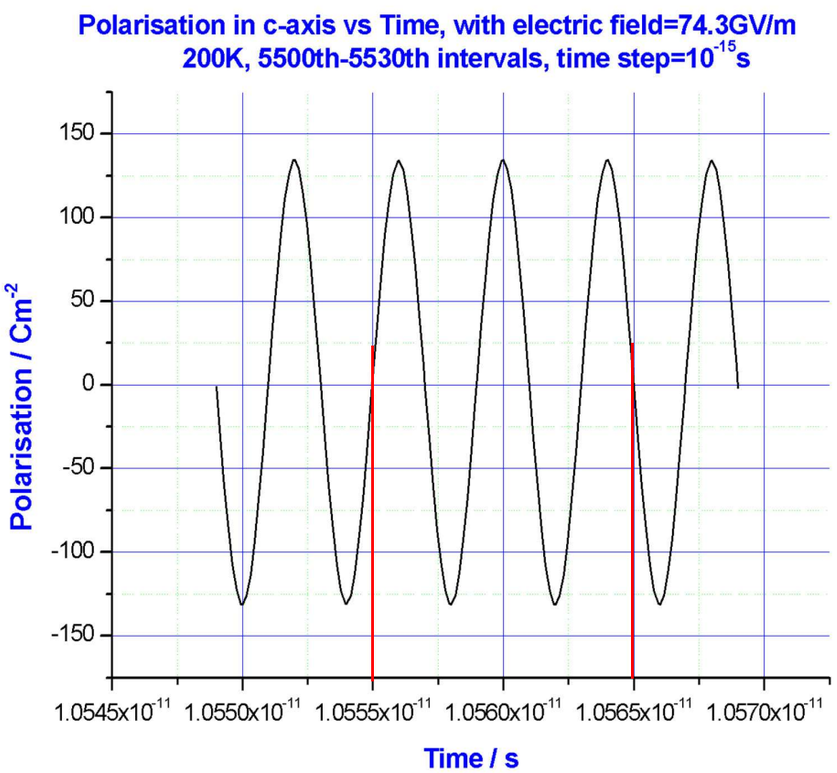

Fig. 13. The polarisation in c-axis (5500^{th}-5530^{th} intervals) with an applied field of 74.3GV/m and at temperature=200K.

Temperature	*Field*	x_c/*Hz*	*w*	*A*
200K	7.43MV/m	4.9725×10^{10}	9.5740×10^{10}	1.2542×10^{25}
	74.3MV/m	7.6060×10^{10}	7.6709×10^{10}	1.4691×10^{24}
	371.5MV/m	8.2752×10^{10}	8.1569×10^{10}	3.1800×10^{23}
	743MV/m	6.0352×10^{10}	1.4819×10^{11}	3.0551×10^{23}
	7.43GV/m	6.8566×10^{10}	1.6000×10^{11}	1.6091×10^{23}
	74.3GV/m	X	X	X
250K	7.43MV/m	6.8981×10^{10}	6.0862×10^{10}	1.5521×10^{25}
	74.3MV/m	7.7697×10^{10}	4.5186×10^{10}	1.5553×10^{24}
	371.5MV/m	7.2492×10^{10}	1.2669×10^{11}	5.1734×10^{23}
	743MV/m	9.0780×10^{10}	1.3829×10^{11}	3.1967×10^{23}
	7.43GV/m	6.2830×10^{10}	2.6115×10^{11}	2.2998×10^{23}
	74.3GV/m	X	X	X
273K	7.43MV/m	8.0000×10^{10}	8.5186×10^{10}	1.0223×10^{25}
	74.3MV/m	6.8439×10^{10}	5.0805×10^{10}	8.7585×10^{23}
	371.5MV/m	2.6842×10^{10}	1.5083×10^{11}	5.9509×10^{23}
	743MV/m	8.6971×10^{10}	7.0597×10^{10}	1.5142×10^{23}
	7.43GV/m	7.7340×10^{10}	1.1147×10^{11}	1.3679×10^{23}
	74.3GV/m	X	X	X
297K	7.43MV/m	4.9078×10^{10}	6.2072×10^{10}	7.0296×10^{24}
	74.3MV/m	8.3584×10^{10}	8.0137×10^{10}	1.7449×10^{24}
	371.5MV/m	4.4657×10^{10}	1.0050×10^{11}	4.5638×10^{23}
	743MV/m	8.8021×10^{10}	8.5461×10^{10}	1.3662×10^{23}
	7.43GV/m	7.8825×10^{10}	1.2695×10^{11}	1.2511×10^{23}
	74.3GV/m	X	X	X
373K	7.43MV/m	3.1715×10^{10}	2.0310×10^{11}	3.7451×10^{25}
	74.3MV/m	7.5239×10^{10}	8.1134×10^{10}	1.9478×10^{24}
	371.5MV/m	6.5725×10^{10}	9.5740×10^{10}	5.4199×10^{23}
	743MV/m	7.9450×10^{10}	1.3905×10^{11}	2.8229×10^{23}
	7.43GV/m	8.2974×10^{10}	8.7608×10^{10}	1.4814×10^{23}
	74.3GV/m	X	X	X

Table 1. The values for the parameters used (x_c, w and A) for the curve fitting for the imaginary part of the susceptibility.

4. Discussion

4.1 Position and trajectories of movement for the sodium ions

Five different temperatures (200K to 373K) have been set as an initial condition but even at the highest temperature 373K, the sodium ions still have not gained enough energy to leave the equilibrium positions for the next available sites in the absence of an electric field. A comparison of the average position for the first and second sodium ions at 200K and 373K is shown in the figure 14. At 373K, the sodium ions have more energy as the fluctuations are bigger compared to the average positions at 200K, but the sodium ions still do not have enough energy to go into the next available site.

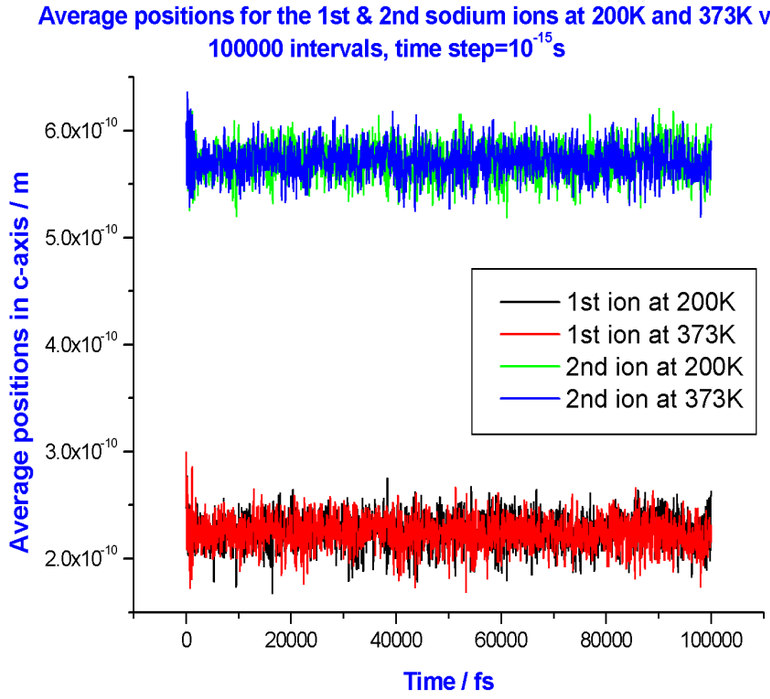

Fig. 14. A comparison of the average positions along c-axis for the first and second sodium ions at 200K and 373K as a function of time.

The next part of the research was to introduce the electric field to the hollandite model. The field was applied from 5001th interval to 100000th interval; it was clearly shown in figure 6 that the fluctuations of the sodium ions increase dramatically at 5001th interval. This is due to the extra energy obtained by the sodium ions from the applied field. In figure 6, take the sixth sodium (pink) for example; it gained enough energy from the applied field to hop into the next available site, which is the next cavity. It then vibrates in this new site for about 2000 intervals until it gained enough energy to hop back to the original cavity. This can be seen in figure 15. From the conservation of energy, in a closed system; the total energy is constant although energy may be transferred between kinetic and potential energy and from one group of sodium ions to another. In the case of the hollandite model, the energy is being swapped around between the sodium ions and this is clearly shown in the figure 16. Only three sodium ions have been shown here, the rest of the sodium ions would behave in a similar way.

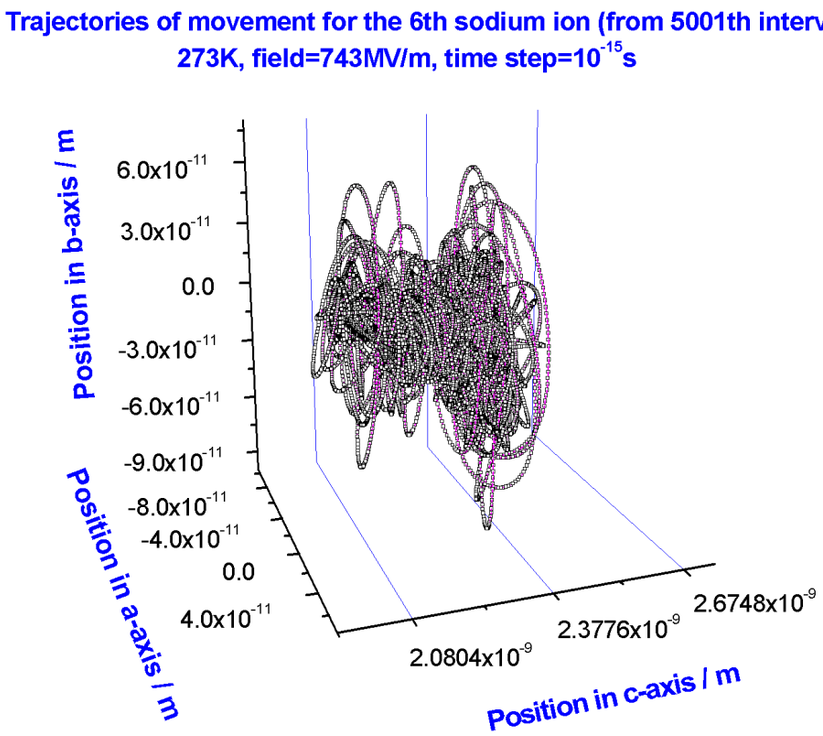

Fig. 15. Trajectories of movement in three-dimensions of the 6th sodium ion in the hollandite model with field of 743MV/m.

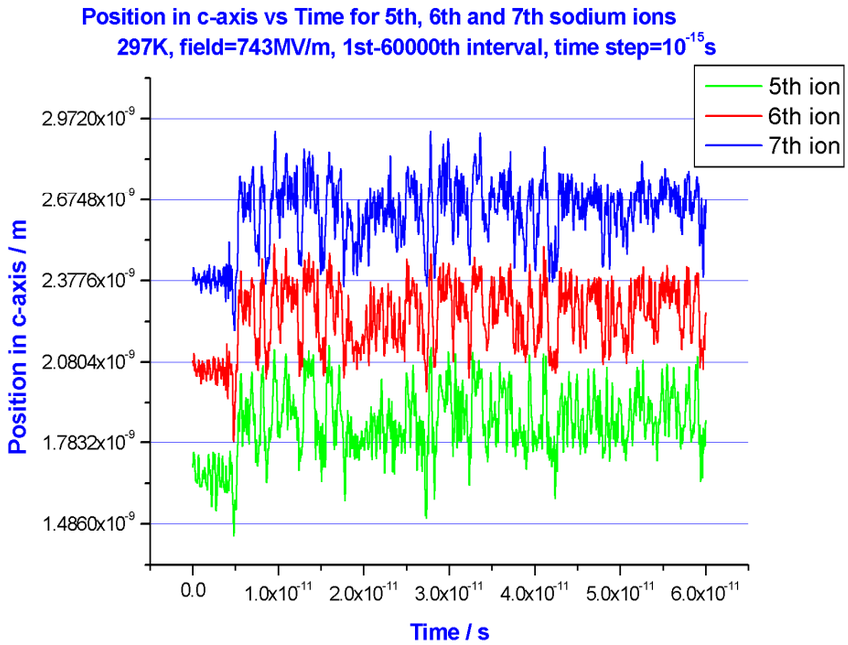

Fig. 16. A comparison of the position in c-axis for the 5th, 6th and 7th sodium ions with field of 743MV/m. The light blue line represents the position of the cavity.

Figure 17 shows that when the dc-field was applied at 5001th interval, the sixth sodium ion starts to gain energy to move into the next empty site. With the applied field of 743MV/m, the sodium ion hops into the next cavity almost as soon as the field is applied, whereas with a lower applied field which is 7.43MV/m, about $9x10^{-12}$ s is needed for the first hop of the sodium ion. As the electric field increases, the number of hops into the neighbouring sites increases as well.

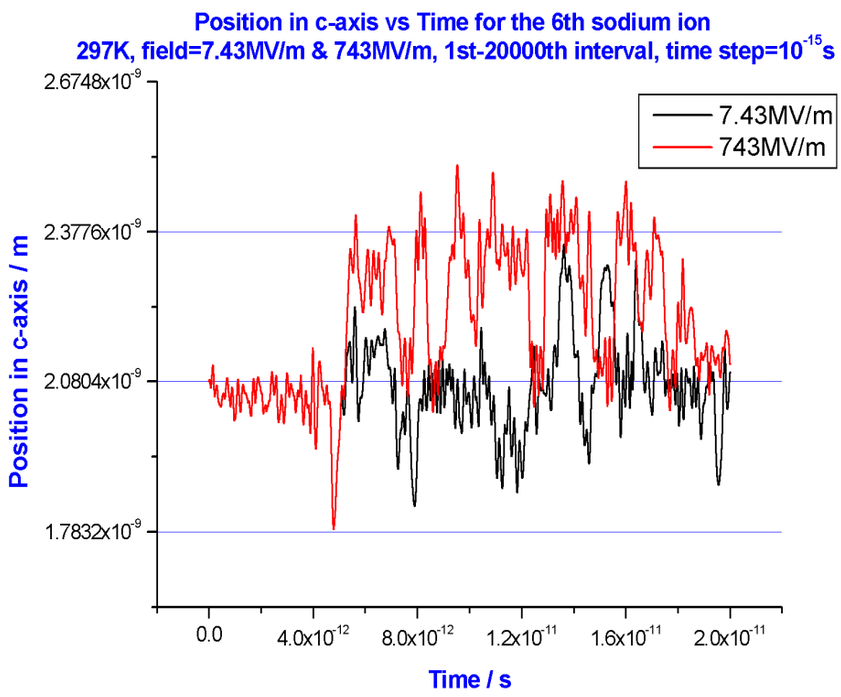

Fig. 17. A comparison of the position in c-axis for the 6th sodium ion with field of 7.43MV/m and 743MV/m. The light blue line represents the cavity.

This movement of the sodium ion is like a dipole moving around, as the sodium ion represents the positive part and the ions at the lattice site that formed the cage is the negative part. A relaxation behaviour would usually be expected to be obtained as the sodium ions hopping between equilibrium positions are like re-orienting dipoles.

4.2 Frequency dependence of χ' and χ"

Frequency dependence of χ' and χ" for a range of temperature and a range of field were obtained from the FFT procedure. The values for the frequency χ'(f) and χ"(f) obtained in our simulations are too high and this is because the hollandite model used (1 tunnel with 60 layers) is only a small section of the whole crystal. If a bigger model had been considered, the average displacement of the ions would be much smaller because the movement of the sodium ions are affected by the sodium ions in the other tunnels, and a smaller polarisation and smaller value of χ'(f) and χ"(f) would be obtained.

From the χ'(f) obtained (figure 9); it is clearly shown that χ'(f) is not a relaxation response as part of χ'(f) gives negative values. Hence the results obtained for χ'(f) and χ"(f) would be more

likely to relate to a resonance response. The peak frequency for $\chi''(f)$ is in the range of ($2.7x10^{10}$ – $8.8x10^{10}$ Hz). Ions hopping between equilibrium sites usually give a relaxation response, whereas in the case of hollandite model, a resonance response is obtained. What seems to be happening is that the movement of the sodium ions between sites change the vibration of the other sodium ions, so that the vibrations of each sodium ion in a group is coupled together and the hopping of one them to a new site destroys the group motion and acts like a damping effect on the resonance that is due to it, i.e. the motion of the system of dipoles behaves like a damped libration. This gives a good agreement to the prediction by Fröhlich (Fröhlich, 1958) who suggested that the absorption due to displacement of charges bound elastically to an equilibrium position is of resonance character, although in our case the ability of the sodium ions to displace from site to site adds a visco-elastic dimension to the situation.

In order to fit $\chi'(f)$ an additional resonance of amplitude y_0 can be added in equation 6. y_0 relates to the isolated higher frequency oscillations which had been removed by the smoothing process. Figure 18 below shows the real and imaginary parts of the susceptibility with a smoothing level of 2000 (that is 2000 points have been used as the number of data points considered to be smoothed at a time). It is clearly shown that adding a higher frequency resonance improves the fit to the data, and hence that oscillations in the form of additional resonance absorptions are present. The lowest resonance absorption was at the same position as in the results shown in figure 9.

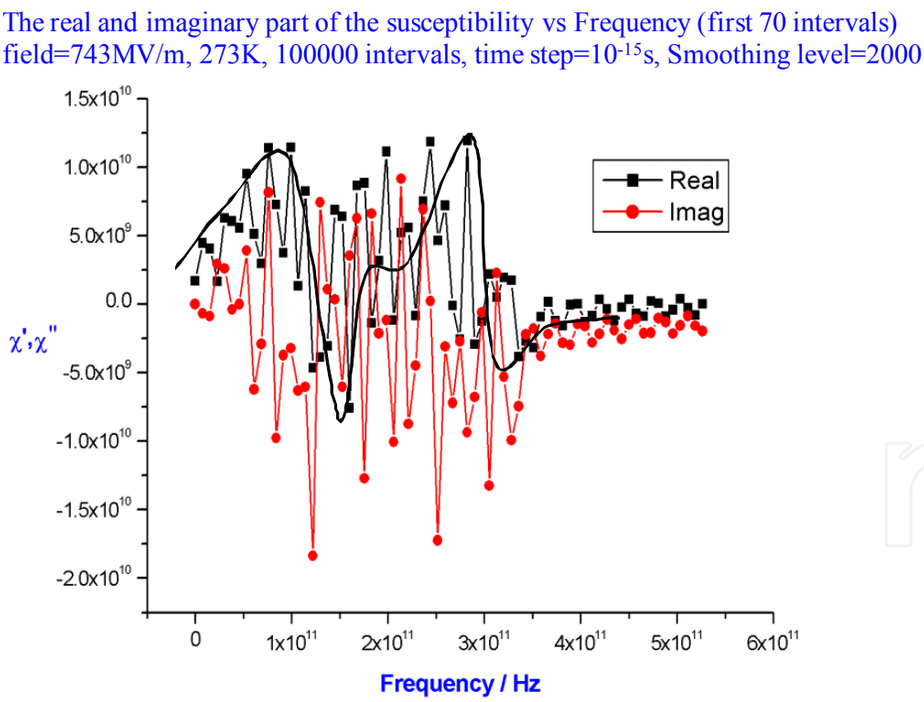

Fig. 18. The real and imaginary parts of the susceptibility as a function of frequency with an electric field of 743MV/m.

A single Lorentzian function does not fit both $\chi'(f)$ and $\chi''(f)$ well. Equation 7 does not fit $\chi''(f)$ well as it gives a symmetrical peak curve whereas $\chi''(f)$ is not symmetrical. The simulated $\chi''(f)$ data shows a steeper gradient at frequencies below the resonance absorption compared to the

fitted curve (equation 7). Similarly, equation 6 would not fit $\chi'(f)$ as equation 6 would give a symmetrical plot in magnitude where the maximum and the minimum points have the same value in magnitude but different sign. This is understandable as the Lorentzian function is generated when a single oscillator is damped by the surroundings whereas in the hollandite model the movement of the sodium ions between sites depend on the other sodium ions. The hopping of any of the sodium ions would damp the libration of the rest of the sodium ions. Hence, there is no specific frequency, which can be considered as a resonance since the number of sodium ions taking part in a group oscillation can change, with each number involved having a different group-oscillator frequency and hence different resonance frequency. However, the Lorenzian function has been used because there is no general non-linear frequency dependent expression available and we have to try to find some ways of expressing the results. As shown in figure 18 increasing the number of resonances improves the fit and hence we can expect when enough resonances have been included a good fit will be obtained within the limitations imposed by the time window of the simulation.

4.3 Temperature dependence

Simulations have been carried out for a range of electric field between 7.43MV/m and 7.43GV/m and temperatures between 200K and 373K. The absorption peak frequency, which is also the resonance frequency, and the resonance peak height, has been plotted as a function of temperature for a range of electric field in figures 19 and 20.

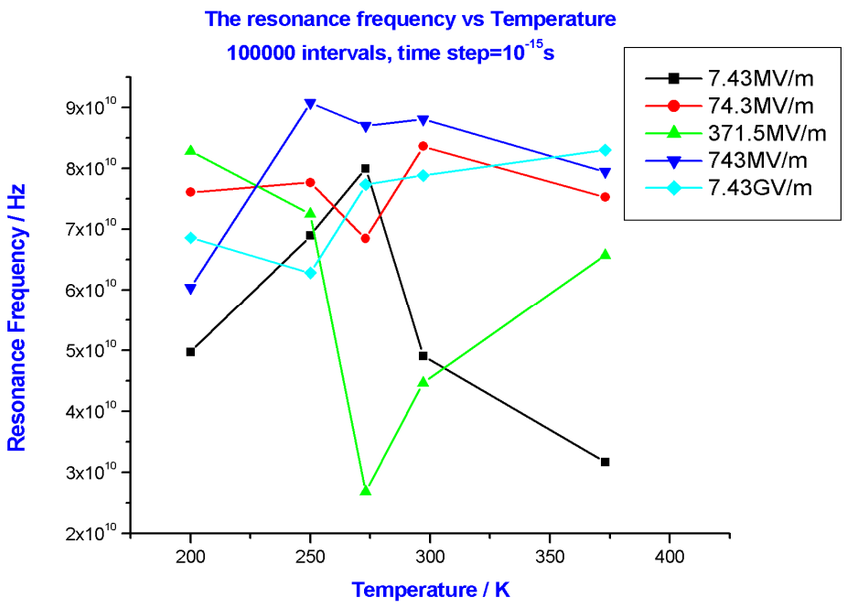

Fig. 19. The resonance frequency as a function of temperature for a range of electric field (7.43MV/m – 7.43GV/m).

From figure 19 the resonance frequency is independent of temperature for all the different electric field applied, and from figure 20 the resonance peak height does not change significantly as the temperature increases. This behaviour is not what would be expected of a dielectric relaxation but is what would be expected from the oscillatory behaviour of groups of sodium atoms whose vibrations are coupled together, where the temperature

would affect the lifetime of the group oscillation and hence the half-width of the peak but not the frequency of the group oscillation.

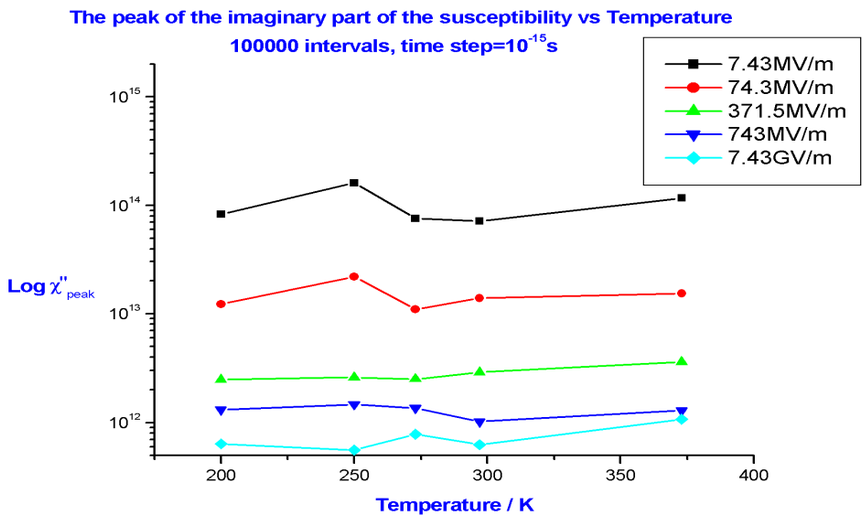

Fig. 20. The peak of the imaginary part of the susceptibility as a function of temperature for a range of electric field (7.43MV/m – 7.43GV/m).

4.4 Poley absorption

The imaginary part of the susceptibility has been plotted for a range of electric field (7.43MV/m – 7.43GV/m) at 297K as shown in figure 21 below. When the applied field gets higher, χ'' becomes smaller. This indicates that the higher the field, the less ions are involved in the group site-libration modes and more in damping (i.e. hopping between sites). The hopping of the sodium ions damp the libration of other sodium ions similar to the friction between the disc and annulus damps the libration in the Itinerant Oscillator (IO) model (Coffey et al., 1987).

This IO model does not explain the process that happens in the hollandite model well enough as the IO model is a harmonic model and does not take into account the effect of molecular translations upon the potentials and forces controlling the motion, a factor that our molecular dynamics simulation have shown to be important. The periodic potential model (Vij & Hufnagel, 1985; Praestgaard & van Kampen, 1981) is also not a good approximation for the same reason. On the other hand, the process in the hollandite model has a good agreement with the cluster model presented by Dissado and Alison (Dissado & Alison, 1993), where the cluster model takes into account the translations of the dipole. The displacements (translations) of the solute molecule was affected by the positions of its surrounding solvent molecules (solvent cage) and vice versa to bring the group (cluster) into an equilibrium configuration. This will cause the deformation of the solvent cage so that reorientations of the solute dipole will also involve reorganisation of the solvent cage deformations. A parameter n was defined such that when n=0 the solute did not deform the cage and its dipole reorientation was overdamped giving a relaxation peak with the vibrations of the solvent providing the viscous damping. When n=1 the solute and solvent formed a single cooperative system giving a Poley absorption and no relaxation peak. When

0<n<1, the solute motions were partitioned between the Poley absorption and relaxation peak. In our model the sodium ion system forms both solute (with ions able to hop to new sites) and solvent (with ions vibrating around their equilibrium sites). The surrounding lattice is held rigid and cannot be involved in the cage motions.

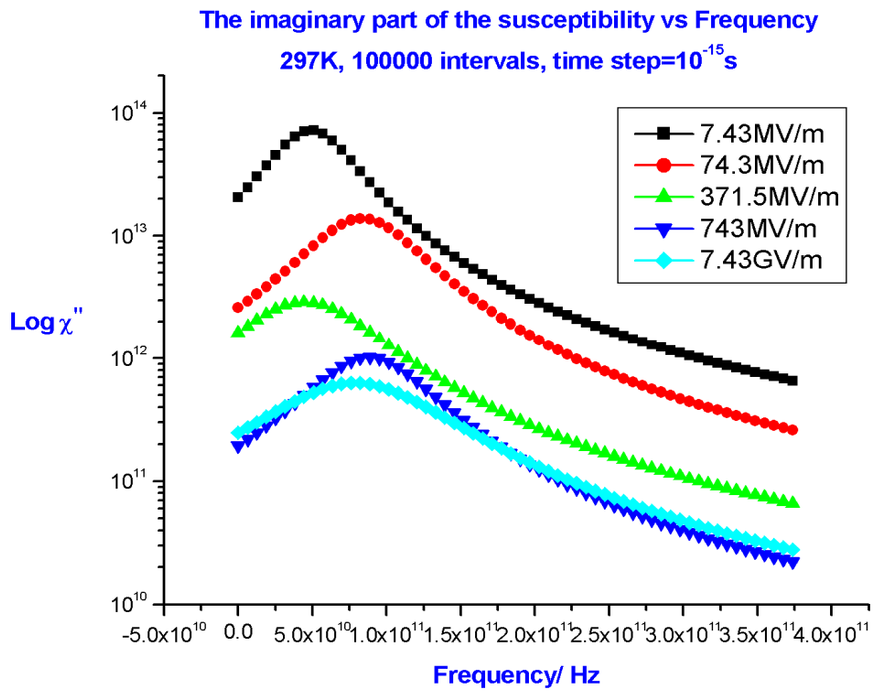

Fig. 21. The imaginary part of the susceptibility has been plotted for a range of electric field (7.43MV/m – 7.43GV/m) at 297K.

The kinetic energy of the sodium ions (defined by the temperature) would initially cause the librations of the sodium ions under the action of the forces from the ions in the fixed lattice sites. Forces from the environment (which is the other sodium ions with respect to a particular sodium ion, and the ions in the lattice sites) causes the sodium ions themselves to produce a force acting on each other, so that the displacement of each sodium ion would be adjusted according to the new equilibrium configuration at each interval, and hence translations changing the potentials occurs on top of the librations. The cluster model would suggest that since all sodium ion motions act cooperatively the parameter n≈1 and there would be a Poley peak with either a weak relaxation peak or none at all. Although the simulations have not been carried through to times longer than ~10^{-10}s, this seems to be what is happening, as the ion motions include both hopping and vibration and give just a damped resonance without any evidence of a relaxation peak.

At 297K, the resonance frequency is in the range of about $4.5x10^{10}$ – $8.8x10^{10}$ Hz for a range of electric field (7.43MV/m – 7.43GV/m). Poley (Poley, 1955) predicted that there is a significant power absorption in dipolar liquids at the ambient temperature in the 1.2 - 70 cm^{-1} ($3.6x10^{10}$ – $2.1x10^{12}$ Hz) region and Davies (Davies et al, 1969) named the broad peak as 'Poley absorption'. The absorption peaks obtained for the hollandite model lie at the lower end of Poley's prediction range. This absorption is due to the libration of the sodium

ions confined to the host structure undergoing displacement under the effect of electric field. The absorptions calculated lie below the resonance frequency of a single sodium ion, which defines the edge of the quantum region. They correspond to coupled displacements of sodium ion groups. It would be reasonable to assume that our calculated absorption corresponds to what would be the Poley absorption for this material. A similar process happens in ice clathrate materials as shown by Johari (Johari, 2002), where an absorption peak was seen in the far-infrared region ($7.5x10^{11}$ and $1.14x10^{12}$ Hz) and was contributed by the rotational oscillation of the tetrahydrofuran molecule, while confined to the cages of the ice clathrate crystal.

From figure 19, the resonance frequency is independent of temperature for all the different electric field applied. This is different from the deduction made by Johari (Johari, 2002) on the ice clathrate crystal and Nouskova et al (Novskova et al., 1986) on the model of a restricted rotator where the resonance frequency decreases with the increase in temperature due to the increase of the libration magnitude. From figure 20, the resonance peak height does not change much as the temperature increases. This is also different from the deduction made by both Johari (Johari, 2002) and Nouskova (Novskova et al., 1986). Johari reported that the resonance peak height increases with the increase in temperature whereas Nouskova said that the resonance peak height decreases with the increase in temperature. In our hollandite model, the sodium ion group motions take place in a rigid lattice unlike the experimental situation for ice clathrates. Therefore the libration amplitude of an individual sodium ion dipole is unaffected by temperature and the oscillation frequency of a specific group should not be affected unlike the situation in (Johari, 2002; Novskova et al., 1986). The resonance peak magnitude will be dependent upon the number of sodium ions taking part in a coupled group oscillation at a specific frequency and this will not be affected by temperature. The effect of temperature in our model is expected to lie in the half-width of the absorption peaks, since this is due to the hopping of sodium ions between oscillating groups.

4.5 Group oscillation at very high field

From figure 13, it is clearly shown that at high electric field, which is 74.3GV/m for the hollandite model, all the sodium ions were driven by the field to move as a group and show a single frequency vibration. The period of the oscillation is $4x10^{-15}$s. Since we use specular boundary conditions for the tunnel (i.e. the tunnel ends are reflective) this oscillation period is what would be expected if the sodium ions moved as a whole and were reflected from the boundaries after the first and third time-steps (i.e at 90 degree and 270 degree phases in the cycle). In the case of a smaller field, the sodium ion would just hop between empty sites next to the original site where it belongs. At bigger fields the sodium ions would have enough energy to move to the empty sites located furthest away. Figure 22 shows an example of three sodium ions in a tunnel. When the applied field is small, the sodium ions will hop between the available empty sites next to them. The only available site for Ion1 is the one on its right, whereas Ion2 and Ion3 will have two available sites to go to and this depends on the direction of the force acting on that particular sodium ion at that moment. As shown in Figure 21 increasing the field reduces the number of sodium ions taking part in coupled local group site-motions (reduced peak amplitude) in favour of sodium ion hopping between sites. For this reason a trend towards higher resonance frequencies and broader

peaks (i.e. higher damping) can be expected. When the applied field is high enough all the sodium ions will take part in hopping between sites, and the field will force all the sodium ions to move to the furthest available sites as shown in figure 22c. The reflective boundary condition at the two ends of the tunnel cause the sodium ions to vibrate between the two ends and this coherent group oscillation was generated. It can be speculated that this behaviour corresponds to a flow of sodium ions (i.e. a sodium ion dc current) when the boundaries regenerate the sodium ion concentration as would an ion exchange membrane.

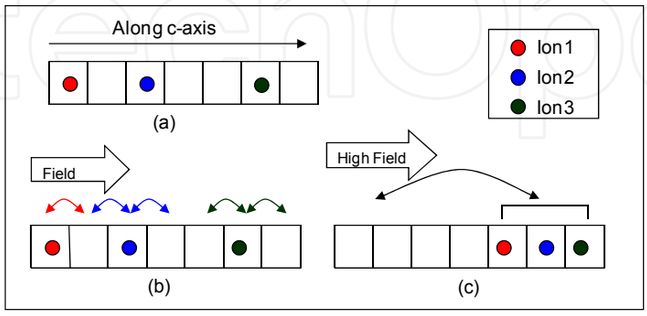

Fig. 22. The position of three sodium ions along c-axis (a) without electric field (b) with low electric field (c) with high electric field. The square denotes the available sites for the sodium ions to move to.

The oscillatory motion is of frequency 2.5x10^{14} Hz and this falls into the infrared frequency region. With a longer tunnel, a higher electric field would be needed to give a coherent group oscillation, as higher force is required to push all the sodium ions to the furthest distance. When all the sodium ions move to one end of the tunnel under the high field, it is just like ALL the dipoles being forced to align in one direction by the electric field, i.e. it is a state of motion that cannot exist without the presence of the field and is thus a non-linear response.

The motion of a group of charges as a whole in the Coulomb field of their counter charges defines a plasma oscillation, and it has a natural frequency that would apply for the sodium ions in an infinitely long tunnel. This plasma oscillation frequency is given in equation 8 below (Ziman, 1960),

$$\omega_p = 2\pi f_p = \sqrt{\frac{ne^2}{m_{Na}\varepsilon_0}} \tag{8}$$

where m_{Na} is the mass for the sodium ion, which is 3.81361x10^{-26} kg, e is the electron charge, ε_0 is the permittivity of free space and n is the concentration of sodium ions (number of sodium ions in a volume of 1m^3). The plasma oscillation frequency that we could expect for our Hollandite model in the absence of the reflective boundaries can be obtained by calculating n as follows: The Hollandite model consists of 60 layers with 24 sodium ions, the volume 1.54475x10^{-27} m^3 is the volume for the 24 sodium ions (Khoo, 2003). The average *volume* for one sodium ion is:

$$volume = \frac{1.54475 \times 10^{-27}}{24} = 6.4365 \times 10^{-29}\ m^3 \tag{9}$$

and n becomes

$$n = 1 / volume = 1.5536 \times 10^{28}\ m^{-3} \tag{10}$$

Substituting equations 9 and 10 into equation 8, the obtained f_p is 5.469x10^{12} Hz. This value is the upper limit for the group oscillations that our simulations show occur in the Hollandite system. The estimated plasma frequency is much lower than the high-field group oscillation frequency (~1/46), but is ten times higher than the frequency of the χ''_{peak} calculated for lower field. This is consistent with an interpretation of the simulations at low fields in which local site vibrations of the sodium ions (equivalent to dipole librations) are coupled together but cannot extend to all the sodium atoms because hopping of an ion between sites destroys the coupled motion, thus giving oscillation frequencies below the plasma oscillation limit. High fields produce a field driven coupled hopping that oscillates the ions between the reflective boundaries at higher frequencies than the plasma oscillation frequency.

5. Conclusions

We have presented a detailed description of the molecular dynamics computational methods applied to the fast-ion conductor Hollandite together with the fundamental concepts needed for interpreting our results. This study focused on the calculation of the sodium ion positions at a range of temperature and electric fields and the resulting frequency dependence of the conductivity mechanism and susceptibility. In the simulation the lattice surrounding the tunnel was held rigid and only the sodium ions in the tunnel were allowed to move. The ac dielectric response was calculated from the rate of change of polarisation, dP/dt, under the action of a dc step-field (i.e. dielectric response function) of 7.43MV/m to 74.3GV/m, at temperatures between 200K and 373K. Our hollandite model shows that the dielectric response due to the motion of the sodium ions in the tunnels behaves approximately like that of polar liquids in the far-infrared frequency region. The susceptibility shows an absorption peak $\chi''(f)_{peak}$ in the frequency region between 4.5x10^{10} and 8.8x10^{10} Hz at 297K. This fitted very well with Poley's prediction of an absorption typically observed in polar liquids in the 1.2 - 70 cm^{-1} (3.6x10^{10} – 2.1x10^{12} Hz) region at room temperature. The frequency dependence of the real and imaginary susceptibility components χ' and χ'' obtained show resonance behaviour. This is due to the vibration of sodium ions coupled together in groups in which the motion of each sodium ion is centred around a local site. This mode of motion is equivalent to the coupled libration of a group of dipoles. Transfer of a sodium ion between sites destroys the coupling for any particular group and acts as a damping on the resonance behaviour associated with its group oscillation. This is in agreement with the prediction by Fröhlich who suggested that the absorption due to displacement of charges bound elastically to an equilibrium position is of resonance character. The absorption peaks in χ'' at the resonance frequency lie between 4.5x10^{10} and 8.8x10^{10} Hz at 297K which matches very well with the Poley absorption which is typically observed in polar liquids in the 1.2 - 70 cm^{-1} (3.6x10^{10} – 2.1x10^{12} Hz) region at room temperature. The resonance frequency and the resonance peak height are independent of temperature. The absorption peak was associated with cooperative motions of the sodium ions

as suggested by the cluster model. The itinerant oscillator model does not allow for such many-body motions. On increasing the applied field χ'' becomes smaller and, more switches of sodium ions between sites are obtained. This indicates that the higher the field, the fewer ions are involved in coupled libration motions and more in damping through hopping between sites. At very high field, which is 74.3GV/m in our simulation, all the sodium ions were driven by the field to move as a group i.e. to transfer collectively from site to site giving a single frequency vibration due to our reflective boundary conditions.

6. References

Byström, A. & Byström, A.M. (1950). The Crystal of Hollandite, the Related Manganese Oxide Minerals, and αMnO_2. *Acta Crystallographica,* Vol.3, pp. 146-154

Chantry, G.W. (1977). Dielectric Measurements in the Submillimeter Region and a Suggested Interpretation of the Poley Absorption. *IEEE Transactions on Microwave Theory and Technique,* Vol.MTT-25, No.6, pp. 496-501

Cheary, R.W. & Dryden, J.S. (1991). Dielectric Relaxation in Hollandite and Rutile. *Philosophical Magazine B,* Vol.64, pp. 709-722

Coffey, W.T.; Corcoran, P.M. & Evans, M.W. (1987). On the Role of Inertial Effects and Dipole-Dipole Coupling in the Theory of the Debye and Far-Infrared Absorption of Polar Fluids. *Proceedings of Royal Society,* Vol.A410, pp. 61-88

Davies, M.; Hill, N.E.; Vaughan, W.E. & Price, A.H. (1969). *Dielectric Properties and Molecular Behaviour,* van Nostrand and Reinhold, London, UK, pp 306

Dissado, L.A. & Alison, J.M. (1993). The Relationship Between the Poley Absorption and Fractional Power Law Relaxation in the Cluster Model. *Journal of Molecular Liquids,* Vol.56, pp. 295-316

Dissado, L.A. & Hill, R.M. (1983). A cluster approach to the structure of imperfect materials and their relaxation spectroscopy. *Proceedings of The Royal Society of London*, Vol. A390, pp131-180

Dissado, L.A. & Khoo, K.L. (2006). The Nature of Terahertz Motions in a One-Dimensional Disordered Structure. *J. Phys. D: Appl. Phys.*, Vol.39, pp. 3882-87

Dixon, M. & Gillan, M.J. (1982). *Computer Simulation in Solids,* Vol.166, pp. 275, Springer-Verlag, Berlin, Germany

Dryden, J.S. & Wadsley, A.D. (1958). The Structure and Dielectric Properties of Compounds with the Formula $Ba_x(Ti_{8-x}Mg_x)O_{16}$. *Transaction Faraday Soc.,* Vol.54, 1574-1580

Fröhlich, H. (1958). *Theory of Dielectrics,* (2^{nd} edition), pp. 131, Clarendon Press, Oxford, UK

Haile, J.M. (1992). *Molecular Dynamics Simulation, Elementary Methods,* John Wiley & Son Inc., Canada

Johari, G.P. (2002). Molecular Inertial Effects in Liquids: Poley Absorption, Collision-Induced Absorption, Low Frequency Raman Spectrum and Boson Peaks. *Journal of Non-Crystalline Solids,* Vol.307-310, pp. 114-127

Jonscher, A.K. (1983). *Dielectric Relaxation in Solids,* Chelsea Dielectric Press Ltd, London, UK

Karpus, M. & Petsko, G.A. (1990). Molecular Dynamics Simulations in Biology. *Nature,* Vol.347, pp. 631-639

Khoo, K.L. (December 2003). *The Construction of Molecular Dynamics Model for the Response of $Na_xCr_xTi_{8-x}O_{16}$ (x=1.7) to Electric Fields of up to 100ps Duration,* PhD Thesis, Department of Engineering, University of Leicester

Khoo, K.L.; Dissado, L.A.; Fothergill, J.C. & Youngs, I.J. (2004). Molecular Dynamics Simulation of High Frequency (10^{10} to 10^{12} Hz) Dielectric Absorption in the Hollandite $Na_x(Ti_{8-x}Cr_x)O_{16}$, *International Conference on Solid Dielectrics,* pp. 550-553, Toulouse, France, July 5-9, 2004

Khoo, K.L.; Dissado, L.A. & Fothergill, J.C. (2007). Molecular Dynamics Simulation on Hollandite $Na_x(Ti_{8-x}Cr_x)O_{16}$: Dependence of DC Conductivity upon Temperature and Concentration, *International Conference on Solid Dielectrics,* pp. 47-50, Winchester, UK, July 8-13, 2007

LMGP-Suite Suite of Programs for the interpretation of X-ray Experiments, by Jean Laugier and Bernard Bochu, ENSP/Laboratoire des Matériaux et du Génie Physique, BP 46. 38042 Saint Martin d'Hères, France, http://www.inpg.fr/LMGP and http://www.ccp14.ac.uk/tutorial/lmgp/

Michiue, Y. & Watanabe, M. (1995a). X-ray Analysis of Sodium Ion Distribution in the One-Dimensional Tunnel of Priderite. *Solid State Ionics,* Vol.79, pp. 116-119

Michiue, Y. & Watanabe, M. (1995b). $Na_x(Ti_{8-x}Cr_x)O_{16}$, Priderite with Sodium Ions in the Tunnel-Structural Study for Stability and Na Ion Transport. *Journal of Solid State,* Vol.116, pp. 296-299

Michiue, Y. & Watanabe, M. (1996). Molecular Dynamics Simulation of Sodium Ions in One-Dimensional Tunnel Structure of Hollandite-Type. *Journal Physics Chemistry Solids,* Vol.57, pp. 547-551

Michiue, Y. & Watanabe, M. (1999). Atomistic Simulation Study of K-Hollandite: Ionic and Dynamics of the Linearly Disordered Solid. *Physical Review B,* Vol.59, No.17, pp. 11298-11302

Novskova, T.A.; Kukebaev, A.M. & Gaiduk, V.I. (1986). One Parameter Model of Dielectric Relaxation in Polar Liquids. *Institute of Radio Engineering and Electronics,* Academy of Sciences of USSR, Vol.29, No.1, pp. 41-54

Poley, J.Ph. (1955). Microwave Dispersion of some Polar liquids. *Journal Applied. Science,* Vol.4, pp. 337-387

Praestgaard, E. & van Kampen, N.G. (1981). A Model for Rotational Relaxation and Resonance. *Molecular Physics,* Vol.43, pp. 33-45

Singer, J.; Kautz, H.E.; Fielder, W.L. & Fordyce, J.S. (1973). *Fast Ion Transport in Solids,* pp. 653-663, Amsterdam, Holland

Vij, J.K. & Hufnagel, F. (1985). Advances in Microwave and Submillimeter Wave Dielectric Spectroscopic Techniques and their Application, in *Advances in Chemical Physics: Dynamical Processes in Condensed Matter,* Evans, M.W. (Ed.), Vol.LXIII, pp. 775-837, J. Wiley and Sons, NY

West, A.R. (1988). *Basic Solid State Chemistry,* Wiley, Chichester, UK

Yoshikado, A.; Ohachi, T.; Taniguchi, I.; Onoda, Y.; Watanabe, M. & Fujiki, Y. (1982). AC Ionic Conductivity of Hollandite Type Compounds from 100 Hz to 37.0 GHz. *Solid State Ionics,* Vol.7, pp. 335-344

Ziman, J.M. (1960). *Electron and Phonons. The theory of Transport Phenomena in Solids,* pp. 161-162, Clarendon Press, Oxford, UK

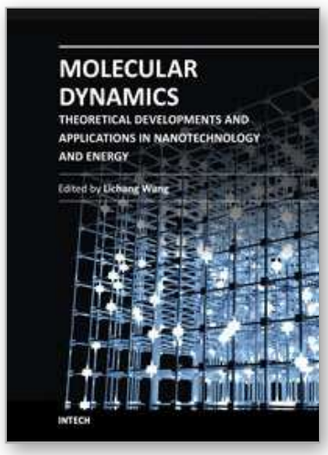

Molecular Dynamics - Theoretical Developments and Applications in Nanotechnology and Energy

Edited by Prof. Lichang Wang

ISBN 978-953-51-0443-8
Hard cover, 424 pages
Publisher InTech
Published online 05, April, 2012
Published in print edition April, 2012

Molecular Dynamics is a two-volume compendium of the ever-growing applications of molecular dynamics simulations to solve a wider range of scientific and engineering challenges. The contents illustrate the rapid progress on molecular dynamics simulations in many fields of science and technology, such as nanotechnology, energy research, and biology, due to the advances of new dynamics theories and the extraordinary power of today's computers. This first book begins with a general description of underlying theories of molecular dynamics simulations and provides extensive coverage of molecular dynamics simulations in nanotechnology and energy. Coverage of this book includes: Recent advances of molecular dynamics theory Formation and evolution of nanoparticles of up to 106 atoms Diffusion and dissociation of gas and liquid molecules on silicon, metal, or metal organic frameworks Conductivity of ionic species in solid oxides Ion solvation in liquid mixtures Nuclear structures

InTech Europe
University Campus STeP Ri
Slavka Krautzeka 83/A
51000 Rijeka, Croatia
Phone: +385 (51) 770 447
Fax: +385 (51) 686 166
www.intechopen.com

InTech China
Unit 405, Office Block, Hotel Equatorial Shanghai
No.65, Yan An Road (West), Shanghai, 200040, China
中国上海市延安西路65号上海国际贵都大饭店办公楼405单元
Phone: +86-21-62489820
Fax: +86-21-62489821

IntechOpen